

# Pitfalls in the ABTS Peroxidase Activity Test: Interference of Photochemical Processes

Andrea Liberato,<sup>†</sup> M. Jesús Fernández-Trujillo,<sup>†</sup> Ángeles Mániz,<sup>†</sup> Marcelino Maneiro,<sup>\*,‡</sup> Laura Rodríguez-Silva,<sup>‡</sup> and Manuel G. Basallote<sup>\*,†,‡</sup>

<sup>†</sup>Departamento de Ciencia de los Materiales e Ingeniería Metalúrgica y Química Inorgánica, Facultad de Ciencias, Universidad de Cádiz, Avda. República Saharaui s/n, Puerto Real, 11510 Cádiz, Spain

<sup>‡</sup>Departamento de Química Inorgánica, Facultad de Ciencias, Campus de Lugo, Universidade de Santiago de Compostela, Avda. Alfonso X s/n, Lugo 27002, Spain

## Supporting Information

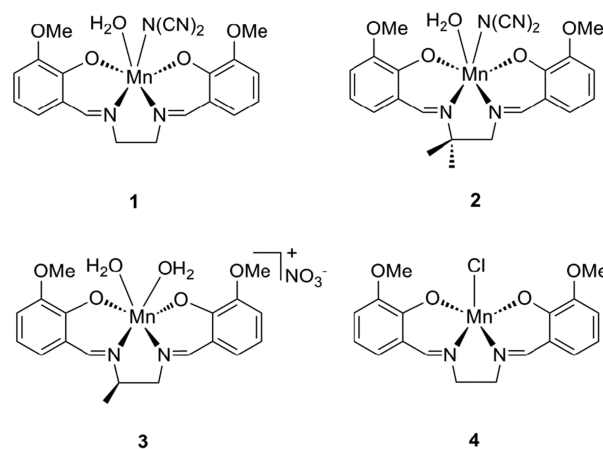
**ABSTRACT:** ABTS (2,2'-azinobis(3-ethylbenzothiazoline)-6-sulfonic acid) oxidation to form its radical cation in the presence of H<sub>2</sub>O<sub>2</sub> is frequently used as a test for determining the peroxidase activity of enzyme mimics. Detailed studies using salen-type Mn(III) complexes show that photochemical processes involving H<sub>2</sub>O<sub>2</sub>, ABTS, and the complex itself can lead to erroneous results. The capability of the complexes to act as •OH scavengers can be also relevant when the mechanism of their biological activity is considered.

Control of H<sub>2</sub>O<sub>2</sub> levels in biological systems by antioxidant enzymes as catalases, peroxidases, and glutathione peroxidases<sup>1</sup> is critical to avoid oxidative stress, which causes numerous diseases and aging.<sup>2</sup> The diammonium salt of 2,2'-azinobis(3-ethylbenzothiazoline)-6-sulfonic acid (ABTS) is a water-soluble trap for radical species commonly used for peroxidase assays<sup>3</sup> with both natural peroxidases<sup>4</sup> and enzyme mimetics.<sup>5</sup> Peroxidase mimics may constitute an exogenous source of peroxidases for living organisms to neutralize overproduction of H<sub>2</sub>O<sub>2</sub>,<sup>6</sup> but they also attract interest in industrial processes under environmentally friendly catalytic methods.<sup>7</sup> Hundreds of compounds have been evaluated by the ABTS test since the 70s,<sup>8</sup> including some reported by us.<sup>9</sup> ABTS is colorless and reacts readily with H<sub>2</sub>O<sub>2</sub> in the presence of a catalyst to yield a green radical cation, ABTS<sup>•+</sup>, with several absorption bands that can be used for quantitative determinations.<sup>10</sup> Although the stability of ABTS and ABTS<sup>•+</sup> may vary depending on the reaction conditions,<sup>11</sup> reproducible results are usually obtained with this method, which allows establishing and comparing the peroxidase-like activity of artificial mimics.

Manganese complexes with salen, and related ligands containing different spacers between the aromatic rings, are ROS scavengers whose catalytic and pharmacological properties have been studied for over 20 years.<sup>6a,12</sup> It is well-established that they protect cells from oxidative damage in animal models and lead to benefits in Alzheimer's and Parkinson's diseases, stroke, motor neuron disease, multiple sclerosis, and excitotoxic neural injury.<sup>13</sup> To gain insight into the kinetic and mechanistic details of the peroxidase-like activity of salen-type Mn(III) complexes, we selected three

artificial mimics (1–3, Chart 1) that differ in their neutral or ionic nature and in the spacers between the phenyl rings.

Chart 1. Structure of Complexes 1–4



These compounds had been previously reported as peroxidase-like catalysts on the basis of the results for the standard ABTS peroxidase test.<sup>9</sup> For comparative purposes, the well-known EUK-134 complex (4), which acts as scavenger for hydrogen peroxide, and has been tested against different oxidative pathologies and commercialized as a potent antioxidant,<sup>6a,12,13c</sup> was also included in the study.

During the course of the work we found that spectral scanning experiments with solutions containing ABTS, H<sub>2</sub>O<sub>2</sub>, and one of the complexes at concentrations typically used in the ABTS test yield systematically different results depending on the instrument used (see Table 1 and the SI). The appearance of the bands typical of ABTS<sup>•+</sup> is observed with any of the instruments, but the experiments showed that those bands initially increase and then decrease in a slower process. Both the magnitude of the absorbance changes and the time scale drastically depend on the instrument used, as illustrated by the kinetic traces in Figure 1 at wavelengths corresponding to maxima in the spectrum of ABTS<sup>•+</sup>. The time required to achieve the maximum concentration of the radical is only 35 s

Received: September 5, 2018

**Table 1. ABTS<sup>•+</sup> Yield Obtained under Different Illumination Conditions for Solutions with Different Compositions**

compounds <sup>b</sup>	ABTS <sup>•+</sup> yield <sup>a</sup>		
	UV-vis <sup>c</sup>	SF <sup>d</sup>	455 nm filter <sup>e</sup>
1 + ABTS + H <sub>2</sub> O <sub>2</sub>	0.06	0.68, 0.66 <sup>f</sup>	0.64
2 + ABTS + H <sub>2</sub> O <sub>2</sub>	0.08	0.62	0.21
3 + ABTS + H <sub>2</sub> O <sub>2</sub>	0.04	0.68	0.56
4 + ABTS + H <sub>2</sub> O <sub>2</sub>	0.09	0.68	0.35
ABTS	0	0.10	0
ABTS + H <sub>2</sub> O <sub>2</sub>	0.05	0.33	0
ABTS + 1	0	0.58	0.02
ABTS + 2	0	0.35	0.06
ABTS + 3	0	0.26	0.07
ABTS + 4	0	0.38	0.14

<sup>a</sup>Quotient between the maximum concentration of ABTS<sup>•+</sup> and the initial concentration of ABTS. <sup>b</sup>Solvent, acetonitrile with 2.5% of water; initial concentrations, [ABTS]<sub>0</sub> = (1.6–4.8) × 10<sup>-5</sup> M, [complex]<sub>0</sub> = 2.5 × 10<sup>-5</sup> M, [H<sub>2</sub>O<sub>2</sub>]<sub>0</sub> = 0.05 M. <sup>c</sup>Conventional UV-vis spectrophotometer. <sup>d</sup>Stopped-flow instrument. <sup>e</sup>Stopped-flow instrument using a 455 nm cut-on long pass filter. <sup>f</sup>Oxygen-depleted solutions.

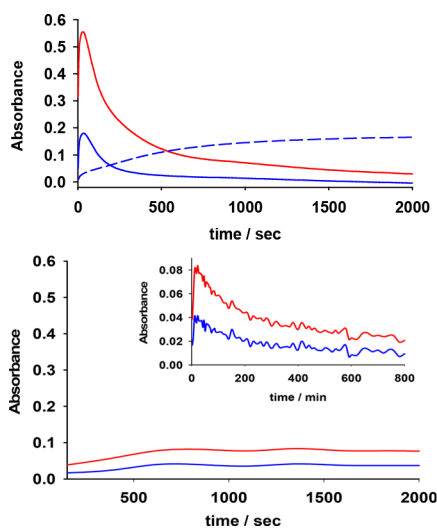


**Figure 1.** Kinetic traces at 400 (red) and 750 (blue) nm obtained for the ABTS peroxidase test using compound 1 with a conventional spectrophotometer (bottom, note the different scales of the main figure and the inset) and with a stopped-flow instrument (top). The blue dashed line corresponds to an SF experiment using a 455 nm cut-on long pass filter. Solvent, acetonitrile with 2.5% of water; temperature, 25.0 °C; initial concentrations, [ABTS]<sub>0</sub> = 3.1 × 10<sup>-5</sup> M, [complex]<sub>0</sub> = 2.5 × 10<sup>-5</sup> M, [H<sub>2</sub>O<sub>2</sub>]<sub>0</sub> = 0.05 M.

with the stopped-flow (SF) instrument, which uses a continuous source of white light, but it increases up to 21 min with the conventional spectrophotometer, which uses a pulsed Xe lamp with a scanning monochromator that reduces the amount of light reaching the sample. In addition, the intensity of the ABTS<sup>•+</sup> bands is higher with the SF instrument. These observations clearly suggest that the striking effect of the instrument used is caused by some photochemical process, which was confirmed by the slower formation of ABTS<sup>•+</sup> in SF experiments using a 455 nm cut-on long pass filter (Figure 1). Nevertheless, the amount of ABTS<sup>•+</sup> formed in the latter experiments is close to that achieved without the filter despite the intensity of UV light being presumably smaller

than in the experiments with the conventional spectrophotometer. The observation of a maximum for the bands of ABTS<sup>•+</sup> is somewhat surprising because it is considered a persistent radical, stable even in solutions containing dissolved oxygen.<sup>14</sup> The negligible effect of oxygen was confirmed in experiments using oxygen-depleted solutions, which yielded results similar to those in the presence of air, both in the amount of ABTS<sup>•+</sup> formed and the time course of its absorption bands. Thus, the disappearance of ABTS<sup>•+</sup> must be caused by its disproportionation<sup>3a</sup> and/or its interaction with other species, probably including H<sub>2</sub>O<sub>2</sub> and/or the metal complex. Actually, it has been reported that disproportionation and overoxidation of ABTS<sup>•+</sup> leads to the red azodication ABTS<sup>2+</sup> that decomposes yielding a complex mixture of products.<sup>15</sup> Those processes have been reported to require several hours for completion, but the SF kinetic traces indicate that they can occur in a much faster time scale, probably because they are also photochemically activated.<sup>16</sup> In any case, the present results indicate that the peroxidase activity estimated with this test depends on both the instrument used and the time at which absorbance readings are taken, which constitutes a serious limitation when the activity of different compounds has to be compared.

For additional information, the behavior of the three reagents involved in the test (ABTS, H<sub>2</sub>O<sub>2</sub>, and the artificial mimic) was tested separately and in pairs. Solutions of the complexes 1–4 do not show detectable spectral changes when subjected to the SF illumination conditions. However, the photochemical generation of <sup>•</sup>OH and other radicals from H<sub>2</sub>O<sub>2</sub> (eq 1) is well-known,<sup>17</sup> and the photochemical generation of ABTS<sup>•+</sup> from ABTS (eq 2) in aqueous solution was reported more recently, although with a lower quantum yield.<sup>14</sup> Despite these reports, the possibility of interferences from photochemical processes in the ABTS peroxidase test is usually ignored. In our case, ABTS solutions only show the formation and subsequent decay of small amounts of ABTS<sup>•+</sup> when the SF instrument is used (Table 1). Solutions containing ABTS and H<sub>2</sub>O<sub>2</sub> yield higher concentrations of ABTS<sup>•+</sup>, which can be explained by considering that the higher quantum yield of H<sub>2</sub>O<sub>2</sub> leads to rapid formation of <sup>•</sup>OH radicals that react with ABTS (eq 3). In any case, the amount of ABTS<sup>•+</sup> formed in the experiments with ABTS, either alone or with H<sub>2</sub>O<sub>2</sub>, is smaller than for solutions containing ABTS, H<sub>2</sub>O<sub>2</sub>, and any of the complexes, thus suggesting participation of the Mn species in the process. This suggestion was confirmed in experiments using mixtures of ABTS and one of the complexes, which showed yields intermediate between those observed for ABTS alone and for solutions containing all three reagents (Table 1).

Significant amounts of ABTS<sup>•+</sup> are formed from binary mixtures of ABTS and the Mn complexes even when the filter is used, which can be interpreted by considering that the Mn complex is photochemically activated (eq 4). Although the high intensity of the ABTS<sup>•+</sup> bands hinders an analysis of the spectral changes corresponding to the Mn complex, it must be pointed out that related Mn(III) complexes have been shown to be photoactive, the greatest activity being observed in the 450–600 nm wavelength range.<sup>18</sup> On the other hand, solutions containing H<sub>2</sub>O<sub>2</sub> and one of the complexes showed spectral changes (Figure 2) that also indicate the occurrence of a photochemical process that leads to disappearance of the complex (Table 2). Again the amount of complex decomposed and the time required for its disappearance are strongly

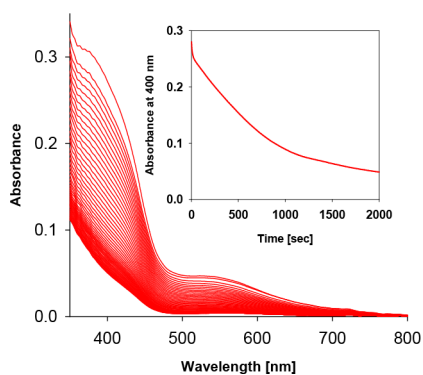


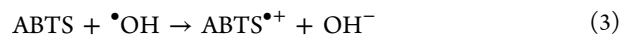
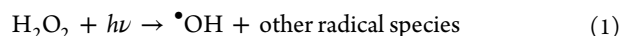
**Figure 2.** Spectral changes observed during 2000 s with a stopped-flow instrument for the reaction of complex **1** ( $4.0 \times 10^{-5}$  M) with  $\text{H}_2\text{O}_2$  ( $2.5 \times 10^{-2}$  M). Solvent, acetonitrile with 2.5% of water; temperature, 25.0 °C.

**Table 2.** Percentage of Complex Decomposed upon Reaction with  $\text{H}_2\text{O}_2$  Using Different Illumination Conditions

compound	complex decomposed <sup>a,b</sup>		
	UV-vis <sup>c</sup>	SF <sup>d</sup>	455 nm filter <sup>d</sup>
1	76	94	0
2	82	88	0
3	33	90	3
4	56	35	7

<sup>a</sup>Solvent, acetonitrile with 2.5% of water; initial concentrations,  $[\text{complex}]_0 = 4.0 \times 10^{-5}$  M,  $[\text{H}_2\text{O}_2]_0 = 0.025$  M. <sup>b</sup>Estimated from the absorbance decrease at 500 nm assuming that the reaction products do not show significant absorption at this wavelength. <sup>c</sup>After 8000 min. <sup>d</sup>After 2000 s.

dependent on the illumination conditions, which suggests that the complexes react with the photochemically generated  $\bullet\text{OH}$  radicals yielding a new  $(\text{MnL})''$  species (eq 1). Interestingly, complex decomposition in the presence of  $\text{H}_2\text{O}_2$  is reduced with the 455 nm filter below the levels observed with the conventional UV-vis instrument (Table 2), whereas the ordering is reversed in the presence of ABTS, the use of the filter leading to higher yields (Table 1). When taken together the whole set of experimental observations indicate the occurrence of a complex series of photochemically triggered radical processes that involve all of the three species used in the ABTS peroxidase test, i.e., ABTS,  $\text{H}_2\text{O}_2$ , and the Mn mimics. As a consequence, the amount of  $\text{ABTS}^{\bullet+}$  estimated is largely affected by the illumination conditions and the time at which absorbance readings are taken, thus introducing severe limitations to the use of the test. At this time it is not possible to determine the  $\text{ABTS}^{\bullet+}$  yield resulting from non-photochemical processes, but the effects of light and of the changes of the absorbance with time can be minimized by avoiding illumination at wavelengths shorter than 455 nm and by measuring absorbance at different times. Although further work is required to shed light on the details,<sup>19</sup> and especially the nature of the  $(\text{MnL})'$  and  $(\text{MnL})''$  species, the present results indicate that formation of  $\text{ABTS}^{\bullet+}$  does not necessarily indicate that the Mn mimic has peroxidase activity but that they can be involved in radical processes. In particular, the capability of these complexes, including EUK-134, to act as  $\bullet\text{OH}$  scavengers must be considered when explaining the mechanism of their biological activity.



## ■ ASSOCIATED CONTENT

### § Supporting Information

The Supporting Information is available free of charge on the ACS Publications website at DOI: 10.1021/acs.inorgchem.8b02525.

Experimental details and selected figures illustrating the experiments used for obtaining the data in Tables 1 and 2 of the main text, including absorption spectra (PDF)

## ■ AUTHOR INFORMATION

### Corresponding Authors

\*E-mail: marcelino.maneiro@usc.es.

\*E-mail: manuel.basallote@uca.es.

### ORCID

Manuel G. Basallote: 0000-0002-1802-8699

### Notes

The authors declare no competing financial interest.

## ■ ACKNOWLEDGMENTS

The authors acknowledge the financial support provided by the Spanish Ministerio de Economía y Competitividad and FEDER funds from the European Union (CTQ2015-71470-REDT and CTQ2015-65707-C2-2-P).

## ■ REFERENCES

- (1) (a) Day, B. J. Catalase and glutathione peroxidase mimics. *Biochem. Pharmacol.* **2009**, *77*, 285–296. (b) Oszajca, M.; Brindell, M.; Orzel, L.; Dabrowski, J. M.; Spiewak, K.; Labuz, P.; Pacia, M.; Stochel-Gaudyn, A.; Macyk, W.; van Eldik, R.; Stochel, G. Mechanistic studies on versatile metal-assisted hydrogen peroxide activation for biomedical and environmental incentives. *Coord. Chem. Rev.* **2016**, *327–328*, 143–165.
- (2) (a) Halliwell, B.; Gutteridge, J. M. C. *Free Radicals in Biology and Medicine*, 4th ed.; Oxford University Press: Oxford, U.K., 2007; p 79. (b) Morry, J.; Ngamcherdtrakul, W.; Yantasee, W. Oxidative stress in cancer and fibrosis: Opportunity for therapeutic intervention with antioxidant compounds, enzymes, and nanoparticles. *Redox Biol.* **2017**, *11*, 240–253. (c) Sosa, V.; Moline, T.; Somoza, R.; Paciucci, R.; Kondoh, H.; Leonart, M. E. Oxidative stress and cancer: an overview. *Ageing Res. Rev.* **2013**, *12*, 376–390.
- (3) (a) Childs, R. E.; Bardsley, W. G. The steady-state kinetics of peroxidase with 2,2'-azino-di-(3-ethyl-benzthiazoline-6-sulphonic acid) as chromogen. *Biochem. J.* **1975**, *145*, 93–103. (b) Makinen, K. K.; Tenovuo, J. Observations on the use of guaiacol and 2,2'-azino-di(3-ethylbenzthiazoline-6-sulphonic acid) as peroxidase substrates. *Anal. Biochem.* **1982**, *126*, 100–108. (c) Organo, V. G.; Filatov, A. S.; Quartararo, J. S.; Friedman, Z. M.; Rybak-Akimova, E. V. Nickel(II) complexes of monofunctionalized pyridine-azamacrocycles: synthesis, structures, pendant arm “on-off” coordination equilibria, and peroxidase-like activity. *Inorg. Chem.* **2009**, *48*, 8456–8468.
- (4) Some recent publications using this method are as follows: (a) Liu, S. W.; Xu, N. H.; Tan, C. Y.; Fang, W.; Tan, Y.; Jiang, Y. Y. A sensitive colorimetric aptasensor based on trivalent peroxidase-mimic DNzyme and magnetic nanoparticles. *Anal. Chim. Acta* **2018**, *1018*, 86–93. (b) Wen, B.; Baker, M. R.; Zhao, H.; Cui, Z.; Li, Q. X.

Expression and characterization of windmill palm tree (*Trachycarpus fortunei*) peroxidase by *Pichia pastoris*. *J. Agric. Food Chem.* **2017**, *65*, 4676–4682. (c) Costa, D.; Passos, M. L. C.; Azevedo, A. M. O.; Saraiva, M. L. M. F. S. Automatic evaluation of peroxidase activity using different substrates under a micro sequential injection analysis/lab-on-valve ( $\mu$ SIA-LOV) format. *Microchem. J.* **2017**, *134*, 98–103.

(5) (a) Lee, Y.; Yoo, S.; Kang, S.; Hong, S.; Han, M. S. An [Mn-2(bmp)]<sup>(3+)</sup> complex as an artificial peroxidase and its applications in colorimetric pyrophosphate and cascade-type pyrophosphatase assay. *Analyst* **2018**, *143* (8), 1780–1785. (b) Mumtaz, S.; Wang, L.-S.; Hussain, S.-Z.; Abdullah, M.; Huma, Z.; Iqbal, Z.; Creran, B.; Rotello, V. M.; Hussain, I. Dopamine coated Fe<sub>3</sub>O<sub>4</sub> nanoparticles as enzyme mimics for the sensitive detection of bacteria. *Chem. Commun.* **2017**, *53*, 12306–12308. (c) Zhao, J.; Wu, Y.; Tao, H.; Chen, H.; Yang, W.; Qiu, S. Colorimetric detection of streptomycin in milk based on peroxidase-mimicking catalytic activity of gold nanoparticles. *RSC Adv.* **2017**, *7*, 38471–38478. (d) Carvalho, R. R.; Pujari, S. P.; Gahtory, D.; Vrouwe, E. X.; Albada, B.; Zuilhof, H. Mild photochemical biofunctionalization of glass microchannels. *Langmuir* **2017**, *33*, 8624–8631. (e) Yang, W.; Wu, Y.; Tao, H.; Zhao, J.; Chen, H.; Qiu, S. Ultrasensitive and selective colorimetric detection of acetamiprid pesticide on the enhanced peroxidase-like activity of gold nanoparticles. *Anal. Methods* **2017**, *9*, 5484–5493. (f) Kang, S.; Oh, J.; Han, M. S. A colorimetric sensor for hydrogen sulfide detection using direct inhibition of active site in G-quadruplex DNAzyme. *Dyes Pigm.* **2017**, *139*, 187–192.

(6) (a) Doctrow, S. R.; Huffman, K.; Marcus, C. B.; Tocco, G.; Malfroy, E.; Adinolfi, C. A.; Kruk, H.; Baker, K.; Lazarowich, N.; Mascarenhas, J.; Malfroy, B. Salen-manganese complexes as catalytic scavengers of hydrogen peroxide and cytoprotective agents: structure-activity relationship studies. *J. Med. Chem.* **2002**, *45*, 4549–4558. (b) Armogida, M.; Nistisico, R.; Mercuri, N. B. Therapeutic potential of targeting hydrogen peroxide metabolism in the treatment of brain ischaemia. *Br. J. Pharmacol.* **2012**, *166*, 1211–1224. (c) Ophoven, S. J.; Bauer, G. Salen-manganese complexes: sophisticated tools for the analysis of intercellular ROS signaling pathways. *Anticancer Res.* **2010**, *30*, 3967–3979.

(7) (a) Wagner, M.; Brumelis, D.; Gehr, R. Disinfection of wastewater by hydrogen peroxide or peracetic acid: development of procedures for measurement of residual disinfectant and application to a physicochemically treated municipal effluent. *Water Environ. Res.* **2002**, *74*, 33–50. (b) Ullrich, R.; Nüske, J.; Scheibner, K.; Spantzel, J.; Hofrichter, M. Novel haloperoxidase from the agaric basidiomycete *Agrocybe aegerita* oxidizes aryl alcohols and aldehydes. *Appl. Environ. Microbiol.* **2004**, *70*, 4575–4581. (c) Ember, E.; Gazzaz, H. A.; Rothbart, S.; Puchta, R.; van Eldik, R. Mn<sup>II</sup>-A fascinating oxidation catalyst: Mechanistic insight into the catalyzed oxidative degradation of organic dyes by H<sub>2</sub>O<sub>2</sub>. *Appl. Catal., B* **2010**, *95*, 179–191.

(8) (a) Ziplies, M. F.; Lee, W. A.; Bruce, T. C. Influence of hydrogen ion activity and general acid-base catalysis on the rate of decomposition of hydrogen peroxide by a novel nonaggregating water-soluble iron(III) tetraphenylporphyrin derivative. *J. Am. Chem. Soc.* **1986**, *108*, 4433–4445. (b) Eulerling, B.; Schmidt, M.; Pinkernell, V.; Karst, U.; Krebs, B. An unsymmetrical dinuclear iron(III) complex with peroxidase properties. *Angew. Chem., Int. Ed. Engl.* **1996**, *35*, 1973–1974. (c) Nagano, S.; Tanaka, M.; Ishimori, K.; Watanabe, Y.; Morishima, I. Catalytic roles of the distal site asparagine-histidine couple in peroxidases. *Biochemistry* **1996**, *35*, 14251–14258. (d) Wei, H.; Wang, E. Fe<sub>3</sub>O<sub>4</sub> magnetic nanoparticles as peroxidase mimetics and their applications in H<sub>2</sub>O<sub>2</sub> and glucose detection. *Anal. Chem.* **2008**, *80*, 2250–2254. (e) Elbaz, J.; Moshe, M.; Shlyahovsky, B.; Willner, I. Cooperative multicomponent self-assembly of nucleic acid structures for the activation of DNAzyme cascades: a paradigm for DNA sensors and aptasensors. *Chem. - Eur. J.* **2009**, *15*, 3411–3418. (f) Brausam, A.; Eigler, S.; Jux, N.; van Eldik, R. Mechanistic investigations of the reaction of an iron(III) octa-anionic porphyrin complex with hydrogen peroxide and the catalyzed oxidation of diammonium-2,2'-azinobis(3-ethylbenzothiazoline-6-sulfonate). *Inorg. Chem.* **2009**, *48*, 7667–7678. (g) Lanza, V.; Vecchio, G. New

conjugates of superoxide dismutase/catalase mimetics with cyclodextrins. *J. Inorg. Biochem.* **2009**, *103*, 381–388. (h) André, R.; Natálio, F.; Humanes, M.; Leppin, J.; Heinze, K.; Wever, R.; Schröder, H.-C.; Müller, W. E. G.; Tremel, W. V<sub>2</sub>O<sub>5</sub> nanowires with an intrinsic peroxidase-like activity. *Adv. Funct. Mater.* **2011**, *21*, 501–509. (i) Noritake, Y.; Umezawa, N.; Kato, N.; Higuchi, T. Manganese salen complexes with acid-base catalytic auxiliary: functional mimetics of catalase. *Inorg. Chem.* **2013**, *52*, 3653–3662.

(9) (a) González-Riopadre, G.; Bermejo, M. R.; Fernández-García, M. I.; González-Noya, A. M.; Pedrido, R.; Rodríguez-Doutón, M. J.; Maneiro, M. Alkali-metal-ion-directed self-assembly of redox-active manganese(III) supramolecular boxes. *Inorg. Chem.* **2015**, *54*, 2512–2521. (b) Vázquez-Fernández, A.; Bermejo, M. R.; Fernández-García, M. I.; González-Riopadre, G.; Rodríguez-Doutón, M. J.; Maneiro, M. Influence of the geometry around the manganese ion on the peroxidase and catalase activities of Mn(III)-Schiff base complexes. *J. Inorg. Biochem.* **2011**, *105*, 1538–1547. (c) Bermejo, M. R.; Fernández, M. I.; González-Noya, A. M.; Maneiro, M.; Pedrido, R.; Rodríguez, M. J.; García-Monteagudo, J. C.; Donnadieu, B. Novel peroxidase mimics:  $\mu$ -aqua manganese-Schiff base dimers. *J. Inorg. Biochem.* **2006**, *100*, 1470–1478.

(10) (a) Wolfenden, B. S.; Wilson, R. L. Radical-cations as reference chromogens in kinetic studies of one-electron transfer reactions – pulse-radiolysis studies of 2,2'-azinobis(3-ethylbenzothiazoline-6-sulfonate). *J. Chem. Soc., Perkin Trans. 2* **1982**, 805–812. (b) Scott, S. L.; Chen, W. J.; Bakac, A.; Espenson, J. H. Spectroscopic parameters, electrode-potentials, acid ionization-constants, and electron-exchange rates of the 2,2'-azinobis(3-ethylbenzothiazoline-6-sulfonate) radicals and ions. *J. Phys. Chem.* **1993**, *97*, 6710–6714.

(11) (a) Pütter, J.; Becker, R., Eds. *Peroxidases*, 3rd ed.; Verlag Chemie: Deerfield Beach, FL, 1983; Vol. 3. (b) Majcherczyk, A.; Johannes, C.; Huttermann, A. Oxidation of aromatic alcohols by laccase from *Trametes versicolor* mediated by the 2,2'-azinobis(3-ethylbenzothiazoline-6-sulfonic acid) cation radical and dication. *Appl. Microbiol. Biotechnol.* **1999**, *51*, 267–276. (c) Kadnikova, E. N.; Kostic, N. M. Oxidation of ABTS by hydrogen peroxide catalyzed by horseradish peroxidase encapsulated into sol-gel glass. Effects of glass matrix on reactivity. *J. Mol. Catal. B: Enzym.* **2002**, *18*, 39–48. (d) Drozd, M.; Pietrzak, M.; Parzuchowski, P. G.; Malinowska, E. Pitfalls and capabilities of various hydrogen donors in evaluation of peroxidase-like activity of gold nanoparticles. *Anal. Bioanal. Chem.* **2016**, *408*, 8505–8513.

(12) (a) Baudry, M.; Etienne, S.; Bruce, A.; Palucki, M.; Jacobsen, E.; Malfroy, B. Salen-manganese complexes are superoxide dismutase-mimics. *Biochem. Biophys. Res. Commun.* **1993**, *192*, 964–968. (b) Doctrow, S. R.; Huffman, K.; Marcus, C. B.; Musleh, W.; Bruce, A.; Baudry, M.; Malfroy, B. Salen-manganese complexes: combined superoxide dismutase/catalase mimics with broad pharmacological efficacy. *Adv. Pharmacol.* **1997**, *38*, 247–269. (c) Kash, J. C.; Xiao, Y.; Sally Davis, A.; Walters, K.-A.; Chertow, D. S.; Easterbrook, J. D.; Dunfee, R. L.; Sandouk, A.; Jagger, B. W.; Schwartzman, L. M.; Kuestner, R. E.; Wehr, N. B.; Huffman, K.; Rosenthal, R. A.; Ozinsky, A.; Levine, R. L.; Doctrow, S. R.; Taubenberger, J. K. Treatment with the reactive oxygen species scavenger EUK-207 reduces lung damage and increases survival during 1918 influenza virus infection in mice. *Free Radical Biol. Med.* **2014**, *67*, 235–247.

(13) (a) Bani, D.; Bencini, A. Developing ROS scavenging agents for pharmacological purposes: recent advances in design of manganese-based complexes with anti-inflammatory and anti-nociceptive activity. *Curr. Med. Chem.* **2012**, *19*, 4431–4444. (b) Bahramikia, S.; Yazdanparast, R. EUK-8 and EUK-134 reduce serum glucose and lipids and ameliorate streptozotocin-induced oxidative damage in the pancreas, liver, kidneys, and brain tissues of diabetic rats. *Med. Chem. Res.* **2012**, *21*, 3224–3232. (c) Doctrow, S. R.; Liesa, M.; Melov, S.; Shirihai, O. S.; Tofilon, P. Salen Mn complexes are superoxide dismutase/catalase mimetics that protect the mitochondria. *Curr. Inorg. Chem.* **2012**, *2*, 325–334.

(14) Lee, C.; Yoon, J. UV direct photolysis of 2,2'-azino-bis(3-ethylbenzothiazoline-6-sulfonate) (ABTS) in aqueous solution:

kinetics and mechanism. *J. Photochem. Photobiol., A* **2008**, *197*, 232–238.

(15) (a) Kadnikova, E. N.; Kostic, N. M. Oxidation of ABTS by hydrogen peroxide catalyzed by horseradish peroxidase encapsulated into sol–gel glass. Effects of glass matrix on reactivity. *J. Mol. Catal. B: Enzym.* **2002**, *18*, 39–48. (b) Majcherczyk, A.; Johannes, C.; Hüttermann, A. Oxidation of aromatic alcohols by laccase from *Trametes versicolor* mediated by the 2,2'-azino-bis-(3-ethylbenzothiazoline-6-sulphonic acid) cation radical and dication. *Appl. Microbiol. Biotechnol.* **1999**, *51*, 267–276. (c) Venkatasubramanian, L.; Maruthamuthu, P. Kinetics and mechanism of formation and decay of 2,2'-Azinobis-(3-E thylbenzothiazole-6-Sulphonate) radical cation in aqueous solution by inorganic peroxides. *Int. J. Chem. Kinet.* **1989**, *21*, 399–421.

(16) Further evidence on the strong effect of the illumination conditions was obtained in SF experiments at single wavelength using a monochromator and a photomultiplier detector set at wavelengths corresponding to the different ABTS<sup>•+</sup> bands. The ABTS<sup>•+</sup> yields at single wavelength (Table S2) are almost 1 order of magnitude lower than when white light is used. Although those yields are quite similar to those with the conventional spectrophotometer, the absorbance maximum is achieved at times much shorter (c.a. 30 s) thus revealing the occurrence of photochemical processes even under these illumination conditions. As none of the three reagents are expected to be excited at wavelengths as high as 844 nm, those findings suggest that light triggers decomposition of the ABTS<sup>•+</sup> formed by the peroxidase activity of the complex.

(17) (a) Hunt, J. P.; Taube, H. The photochemical decomposition of hydrogen peroxide – quantum yields, tracer and fractionation effects. *J. Am. Chem. Soc.* **1952**, *74*, 5999–6002. (b) Buxton, G.; Wilmarth, W. K. Aqueous chemistry in inorganic free radicals. 5. Use of carbon monoxide as a scavenger for hydroxyl radicals generated by photolysis of hydrogen peroxide. *J. Phys. Chem.* **1963**, *67*, 2835–2841. (c) Goldstein, S.; Aschengrau, D.; Diamant, Y.; Rabani, J. Photolysis of aqueous H<sub>2</sub>O<sub>2</sub>: Quantum yield and applications for polychromatic UV actinometry in photoreactors. *Environ. Sci. Technol.* **2007**, *41*, 7486–7490. (d) Chu, L.; Anastasio, C. Formation of hydroxyl radical from the photolysis of frozen hydrogen peroxide. *J. Phys. Chem. A* **2005**, *109*, 6264–6271.

(18) Ashmawy, F. M.; McAuliffe, C. A.; Parish, R. V.; Tames, J. Water photolysis I. The photolysis of coordinated water in [(MnL(H<sub>2</sub>O))<sub>2</sub>](ClO<sub>4</sub>)<sub>2</sub> (L= dianion of tetradentate O<sub>2</sub>N<sub>2</sub>-donor Schiff-bases) – A model for the manganese site in Photosystem-II of green plant photosynthesis. *J. Chem. Soc., Dalton Trans.* **1985**, 1391.

(19) Another point that requires additional investigation is to determine at which extent the present conclusions can be extrapolated to other compounds. In this sense, preliminary experiments with horseradish peroxidase indicate that formation of ABTS<sup>•+</sup> is much faster than with the present Mn complexes, and experiments with both the conventional spectrophotometer and the SF instrument show its disappearance with time scales that also depend on the instrument used, also affecting estimation of the amount of ABTS<sup>•+</sup> formed.